Tuijin Jishu/Journal of Propulsion Technology
ISSN: 1001-4055
Vol. 46 No. 3 (2025)

Inpainting of Images Via Formation of Patterns

Sadia Kumail Awad

Department of Nursing Techniques, Technical Institute of Al-Diwaniyah, Al-Furat Al-Awsat Technical University, Kufa, Najaf, Iraq

Abstract: In this paper, we introduce a novel image inpainting technique for reconstructing damaged or missing image regions. The method relies on pattern formation, specifically searching for predefined patterns that originate from damaged or lost pixels. Subsequently, these pixels are reconstructed by filling them with colors derived from the observed patterns.

Keywords: *Image inpainting, Cahn-Hilliard equation, inpainting path, path gradient*.

1. Introduction

Inpainting is the art of modifying an image such that the results of changes are not easily detectable by an ordinary observer. The purpose of inpainting is to reconstitute the missing or damaged portions of the image, in which the inpainted region is seamlessly merged into the image [4]. Propagating the image information along lines of equal gray values into the areas to be modified is expressed by the third-order nonlinear PDE [6]. In this paper, the authors explained that good inpainting algorithms should propagate sharp edges in surrounding areas into the damaged parts required to be fill in . Furthermore, a new PDE's model based on the reformation of the Navier-Stokes equations with an isotropic term and a fidelity term is proposed by Bertozi [3]. Cahn and Shen proposed the well-known variational image denoising and segmentation models which was adapted to the inpainting task with a simple modification [8]. This model is based on image denoising model of Rudin, Osher, Fatemi [?]. It propagates sharp edges into the damaged domain as well. But this model does not keep the direction of isophotes continuous across the boundary of inpainting. The Cahn and Shen model [9] have drawbacks. So later, Cahn, Kang and Shen introduced a more complete new variational image inpainting model. Two PDE's models for image inpainting based on the Mumford-Shah model are proposed by Esedoglu and Shen [13], one is a simple modification of the fidelity term, another one is obtained by considering the Euler's elastica approximation. Ballester et.al's model [2] is based on joint interpolation of the image gray-levels and gradient/isophotes directions, smoothly expanding in an automatic fashion isophote lines into the missing data. Other PDE's inpainting models can be found in [10], [12], [14], [15], [16], [19] and [22]. The paper [23] contains a modification on the total variation model. It is based on a new insight into the neighborhood pixels of the damaged areas. In this paper, our suggestion model is based on finding the paths whose the first or the end include in inpainting region. These paths involve almost the same colour. The organization of the chapters are as follows:

In Section 2, some variety of models for image inpainting are explained. In Section 3, our proposed model is introduced and finally in Section 4, some numerical experiments are given to confirm the advantages of proposed model.

2 Some models for image inpainting

Image inpainting is the process of filling a missing or a damaged image based on the information obtained from the surrounding areas. It is in fact a type of interpolation [4, 19].

Let $f(x)$ be a given image in a domain Ω, and $D \subset \Omega$ be the inpainting domain. The inpainting model is to find an image u in Ω such that $u \approx f$ on $\Omega \backslash D$ for a given image f in $\Omega \backslash D$ and find a suitable approximation on D (Figure1).

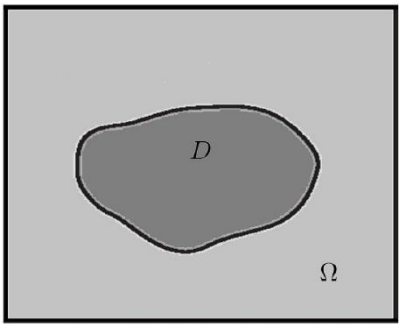

Figure 1: A schematic of the domain Ω and the inpainting region D

In the sequel, we present some variety of image inapinting models:

2.1 The energy method

In order to recover a corrupted images, the selection of suitable degradation operator is very important. Let R be the degradation operator and

$$f = Ru + \eta, \tag{1}$$

where u is the original image (the unknown), f is the observed image and η is a white Gaussian noise. According to the maximum likelihood principle, one can find an approximation of u by solving the least square problem:

$$\min_u \int_\Omega |f - Ru|^2 \, dx. \tag{2}$$

If there exists a minimum u of (2), then we will have the following equation

$$R^*f - R^*Ru = 0, \tag{3}$$

where R^* is the adjoint of R. The equation (3) is an ill-posed problem, therefore, the idea is to add regularization term to the energy. The idea was for Tikhonov and Arsenin [24] whose proposed the minimization problem:

$$F(u) = \int_\Omega |f - Ru|^2 dx + \lambda \int_\Omega |\nabla u|^2 dx, \tag{4}$$

where the first term is referred to as the fidelity term while the second one is a smoothly term and the parameter λ is a positive weightly constant. The value of $inuF(u)$ is characterized by Euler-Lagrange equation,

$$R^*Ru - R^*f - \lambda \Delta u = 0. \tag{5}$$

The equation (5) with the Neuman boundary condition

$$\frac{\partial u}{\partial n} = 0 \text{ on } \partial\Omega, \tag{6}$$

has a unique solution, where n is the unit outward normal vector. Naturally if there exists smoothness in the edges of the image, the condition (6) will satisfies. Adding the regularization term ∇u by the L^2 norm, will be caused to remove the noise, but unfortunately penalizes too much the gradients corresponding to edges. So, one of the solutions can be effective is changing the norm. One of the first works in this direction is due to Rudin, Osher and Fatemi [21], [20] who proposed to use L^1 norm on the regularization term that is referred to as total variation, instead of the L^2 norm. Furthermore, the regularization term can be given in a generalized form by [1]:

$$F(u) = \frac{1}{2}\int_\Omega |f - Ru|^2 dx + \lambda \int_\Omega \phi(|\nabla u|) dx. \tag{7}$$

The Euler-Lagrange equation of (7) reads:

$$R^*Ru - \lambda div\left(\frac{\phi(|\nabla u|)}{|\nabla u|}.\nabla u\right) = R^*f. \tag{8}$$

2.2 Total variation

As we cited in the preceding section, the total variation (TV) inpainting model is represented as follows:

$$\min\left\{\int_{\Omega}|\nabla u|+\frac{\lambda}{2}\int_{\Omega\ D}|u-f|^2dx\right\}, \tag{9}$$

where f is a given image and u is unknown.

The TV regularization term can be interpreted by the existence edges of the image:

$$\min_{u}\int_{\Omega}|\nabla u| \Leftrightarrow \min_{\Gamma_\lambda}\int_{-\infty}^{+\infty}L(\Gamma_\lambda)d\lambda, \tag{10}$$

where $\Gamma_\lambda=\{x\in\Omega: u(x)=\lambda\}$ is the level curves for the gray value λ. and $L(\Gamma_\lambda)$ shows the length of the Γ_λ. The inpainting model has drawbacks that it cannot connect edges over large distances and does not smoothly propagate level curves into the inpainting region. In order to decrease this deficiency, in addition to $|\nabla u|$, the curvature of the level curves are considered

$$\min\int_{\Omega}(a+b\kappa^2)|\nabla u|dx \Leftrightarrow \min_{\Gamma_\lambda}\int_{-\infty}^{+\infty}aL(\Gamma_\lambda)+b\kappa^2(\Gamma_\lambda)d\lambda, \tag{11}$$

where $\kappa=\nabla.\frac{\nabla u}{|\nabla u|}$ is the curvature of level curves Γ_λ of u. So, here it is expected to have a better result than the TV inpainting model [17].

2.3 Binary Cahn-Hilliard inpainting

In this subsection, we explain the modified version of Cahn-Hilliard equation that is used for inpainting of binary images [4].

Let f be the given binary image on domain $\Omega\subset\mathbb{R}^d(d=2,3)$. The aim is to construct the image in the inpainting domain $D\subset\Omega$ in an undetectable way by the evolution of the Cahn-Hilliard equation as

$$\frac{\partial u}{\partial t}=\triangle\left(-\epsilon\triangle u+\frac{1}{\epsilon}F'(u)\right)+\lambda(x)(u-f),\quad in\ \Omega \tag{12}$$

where $F(u)=u^2(u-1)^2$ is a double well-potential and

$$\lambda(x)=\begin{cases}0, & x\in D\\ \lambda, & x\in\Omega\backslash D.\end{cases}$$

If $\lambda(x)=0$, the original Cahn-Hilliard equation will be derived by

$$\frac{\partial u}{\partial t}=\triangle\left(-\epsilon\triangle u+\frac{1}{\epsilon}F'(u)\right). \tag{13}$$

The modified Cahn-Hilliard equation (??) consists of two different flows. Using H^{-1}-norm for the first term of (??) concludes a gradient flow for the Cahn-Hilliard energy as follows:

$$E_1(u)=\int_{\Omega}\left(\frac{\epsilon}{2}|\nabla u|^2+\frac{1}{\epsilon}F(u)\right)dx, \tag{14}$$

while the second term gives a gradient flow under L^2-norm for the fidelity term [4],

$$E_2(u)=\frac{\lambda}{2}\int_{\Omega\backslash D}(u-f)^2dx. \tag{15}$$

Now, E(u)=E_1(u)+ E_2(u), is called modified Cahn-Hilliard energy. Thus the modified Cahn-Hilliard inpainting model (12) gives a superposition of the H^{-1}-gradient flow for $E_1(u)$ and the L^2-gradient flow for $E_2(u)$. The evolution of u can be described as follows:

Outside of the damaged region, u stays close to the given image f. We can control this closeness via the fidelity parameter λ. According to the known image information, the damaged area are filled in. The role of ϵ in equation (12) is important. In the original Cahn-Hilliard equation, ϵ serves as a measure of the transition region between two metals in an alloy, after heating and reaching a steady state. In image processing, ϵ is a measure of the transition region between the two grayscale states (for example between the black and white printed text) [5].

3 The proposed inpainting model

Let $p_0,p_1,p_2,\ldots,p_m$ be the pixels of an image u. We call $\rho=\{p_0,p_1,p_2,\ldots,p_m\}$ the inpaintnig path if the following conditions hold:

1. $p_0 \in D$,

2. $p_1, p_2, \ldots, p_m \in \Omega \backslash D$,

3. $\sum_{i=1}^{m} |u_{p_i} - u_{p_{i-1}}| < \epsilon$,

where u_{p_i} shows the intensity of the image u at the point p_i. The point p_0 can be at the beginning or end of the inpainting path. Without loss of generality, we assume that p_0 is at the beginning of the inpainting path. Let $\pi_j = \{\rho_1, \rho_2, \ldots, \rho_k\}$ be inpainting paths including the point p_0 (see Figure 2). Now, we define the path gradient at the point $p_0 \in D$ for the path ρ_j by

$$\bar{\nabla} u_{\rho_j}(p_0) = \sum_{i=1}^{m} |u_{p_i} - u_{p_{i-1}}|. \tag{16}$$

We calculate the path gradient for each path and define:

$$\bar{\nabla} u_{\rho^*}(p) = \min_{\rho_j} \bar{\nabla} u_{\rho_j}(p_0). \tag{17}$$

Now, we set

$$u(p_0) := \frac{1}{m} \sum_{i=1}^{m} u(p_i),\ p_i \in \rho^* \text{ for } i = 1, \ldots, m. \tag{18}$$

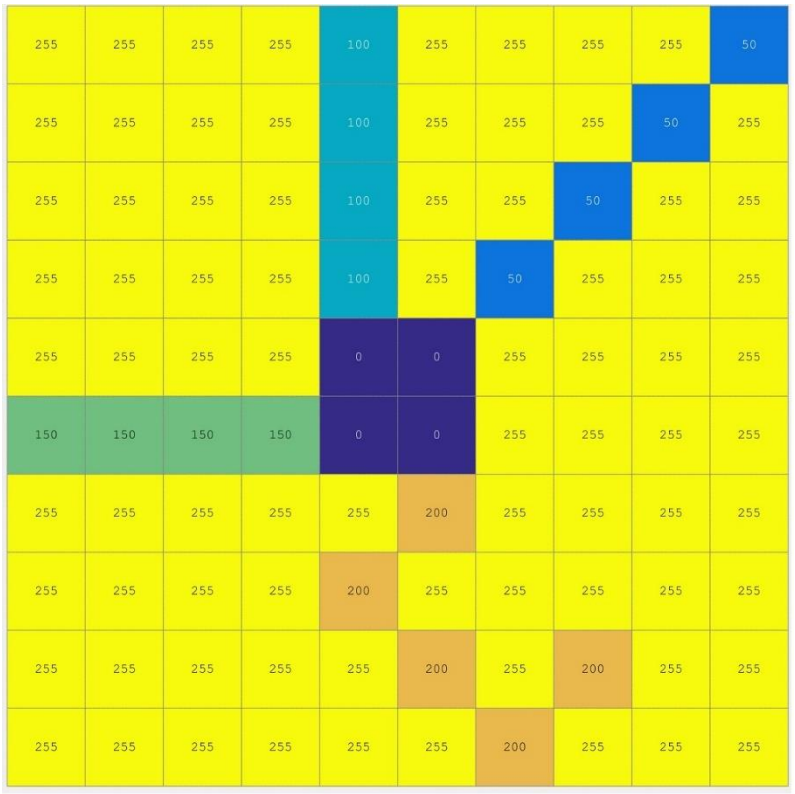

Figure 2: Pixels including zero values show the domain D and pixels including 50, 100, 150 and 200 marked in dark blue, light blue, green and orange respectively, show 4 different paths for 4 pixels in the domain $\Omega \backslash D$.

Algorithm 1 inpaints the region D. Since D is a closed and bounded region, it is clear that Algorithm 1 converges.

Algorithm 1

1 For $i = 1{:}m$ do

2 If $q_i \in D$, then

$p_0 := q_i$

For $j = 1:k$ do

Find $\pi_j = p_1^{(j)}, \dots, p_m^{(j)}$ such that $p_0 \cup \pi_j$ is an inpainting path

$\rho_j := p_0 \cup \pi_j$

Compute $\bar{\nabla} u_{\rho_j}(p_0) = \sum_{i=1}^{m} |u_{p_i}^{(j)} - u_{p_{i-1}}^{(j)}|$

EndFor

Compute $\bar{\nabla} u_{\rho^*}(p_0) = \min_j \bar{\nabla} u_{\rho_j}(p_0)$

$$u(p_0) = \frac{1}{m} \sum_{i=1}^{m} u(p_j)$$

EndIf

EndFor

3.1 The mathematical model of our method

In this subsection, we present a mathematical model for our proposed method. According to modified Cahn-Hilliard equation, our proposed method can be expressed as follows:

$$\min_u J[u] = \int_D |\bar{\nabla} u| dx + \frac{\lambda}{2} \int_{\Omega \setminus D} |f - u|^2 dx, \tag{19}$$

where $\bar{\nabla}$ is the continuous form of (16) and λ is a positive regularization parameter. Therefore, the model can be rewritten by

$$\min_u J[u] = \int_\Omega \chi_\Omega |\bar{\nabla} u| dx + \frac{\lambda}{2} \int_\Omega \chi_{\Omega \setminus D}(x) |f - u|^2 dx, \tag{20}$$

where the characteristic function $\chi_E(x)$ on a domain E is defined by

$$\chi_E(x) = \begin{cases} 1 & x \in E \\ 0 & x \notin E. \end{cases}$$

The Euler-Lagrange equation for the minimization problem (20) reads:

$$-\bar{\nabla}.\left(\frac{\bar{\nabla} u}{|\bar{\nabla} u|}\right) + \lambda \chi_{\Omega \setminus D}(x)(f - u) = 0. \tag{21}$$

In order to solve (21) by an iterative process, we consider the following PDE problem:

$$\frac{\partial u}{\partial t} = \bar{\nabla}.\left(\frac{\bar{\nabla} u}{|\bar{\nabla} u|}\right) + \lambda \chi_{\Omega \setminus D}(x)(f - u). \tag{22}$$

To solve numerically (22), let $u^n(i,j)$ be the value of u in pixel (i,j) at time nh where h is the time step. By forward differences, we have

$$u^{n+1}(i,j) = u^n(i,j) + h\left(\bar{\nabla}.\left(\frac{\bar{\nabla} u^n(i,j)}{|\bar{\nabla} u^n(i,j)|}\right) + \lambda \chi_{\Omega \setminus D}(x)(f(i,j) - u^n(i,j)\right), \tag{23}$$

that is an explicit finite difference scheme.

4 Numerical experiments

In this section, we present some numerical examples to show the efficiency of our proposed method.

Example 1: For the first example, we consider Figure 3(a) that is a 200×200 image of cross in which the inpainting region is shown by gray colour. Figure 3(b) denotes the implementation of the numerical scheme (23) only by 2 iterations. As is seen, the inpainting region is inpainted well.

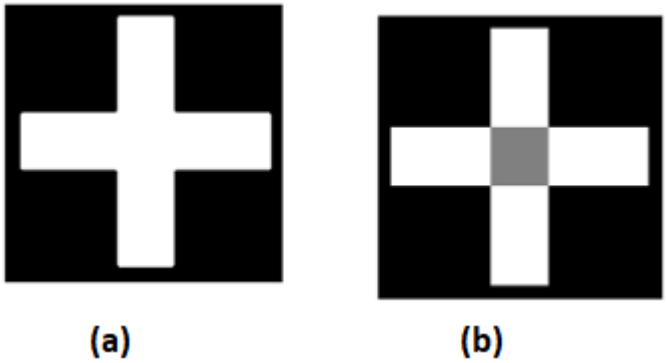

Figure 3: The performance of our approach. (a) A damaged image (b) Running the numerical scheme (23) with 2 iterations.

Let us make a comparison to show how much faster our method is. We compare Figure 3 with a figure "inpainting of a cross" in [5]. They represented the model for inpainting based on the modified Cahn-Hilliard equation for binary image. It is observed that in spite of Figure 3(a), there exist a blurring case in Figure 4(c). So, we see better results in the edges of the image.

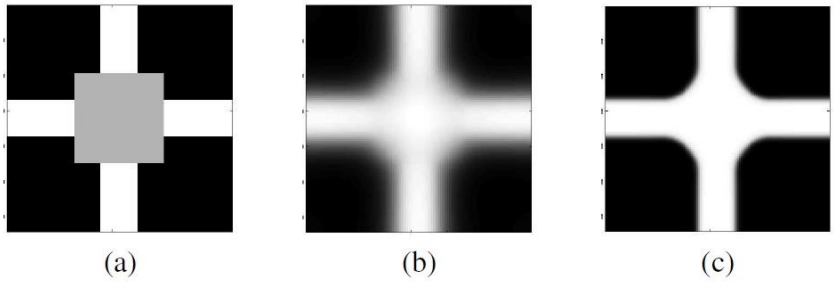

Figure 4: (a) Initial data of cross (inpainting region in gray). (b) Intermediate state at $t = 300$. (c) Steady state at $t = 1000$. (Image domain is 128×128, stripe width is 20 units, initial gap distance is 50 units).

Example 2: Figure 5(a) shows a 200×200 image of a double stripe whose inpainting region is cleared by gray colour. Figures 5(b-d) show the implementation of the numerical scheme (23) in 5, 10 and 14 iterations, respectively. As is seen, the inpainting region is inpainted well.

Figure 5: The performance of our approach on an image. (a) original image and implementation of our proposed method in (b) 5 iterations, (c) 10 iterations and (d) 14 iterations.

As the last example, we compare our method with [5] on the double strip image (Figure 5(a)). Again we observed that our method works well for Figure 5(a).

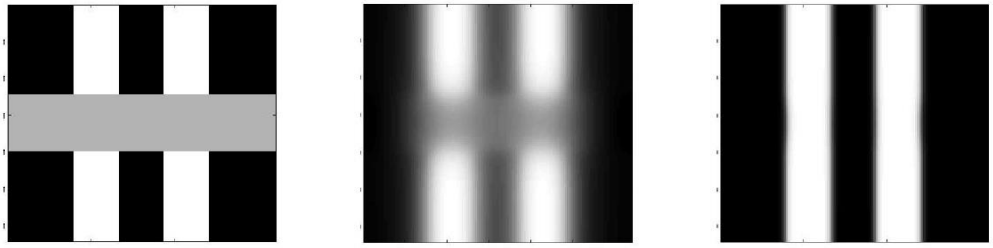

Figure 6: (a) Initial data (inpainting region in gray). (b) Intermediate state at $t = 50$. (c) steady state at $t = 700$. (Gap distance is 30 units, Image domain is 128×128).

Example 3: Figure 7(a) shows a 200×200square image which the inpainting region is black square .Figure 7(b-d) denotes the implementation of the numerical scheme (23) in 5, 8 and 14 iterations, respectively. As is seen, the inpainting region is inpainted well.

Figure 7: The performance of our approach on (a) an original image (b) in 5 iterations, (c) 8 iterations and (d) 14 iterations.

Example 4: Figure 8(a) shows a 200×200 circle image which inpainting region is black square. Figure 8(b-d) denotes the implementation of the numerical scheme (23) in 14, 22 and 29 iterations, respectively. As is seen, although the inpainting region is fairly big, the proposed method inpaints well.

Figure 8: The performance of our approach on (a) an original image (b) in 14 iterations, (c) 22 iterations and (d) 29 iterations.

Refrences

[1] G. Aubert and L. Vese. *A variational method in image recovery*. SIAM Journal of Numerical Analysis, 34(5):1948–1979, October 1997.

[2] C. Ballester, M. Bertalmio, V. Caselles, G. Sapiro, and J. Verdera, *Filling-in by joint interpolation of vector fields and grey levels*, IEEE Trans. Imag. Proc. 10 (2001), 1200–1211.

[3] M. Bertalmio, A. Bertozzi, G. Sapiro, Navier–Stokes, *fluid dynamics and image and video inpainting*. IEEE Comput. Vis. Patt. Recogn., 2001, 1, 355–-362.

[4] M. Bertalmio, G. Sapiro, V. Caselles, and C. Ballester, *Image inpainting*, in Proceedings of the 27th Annual Conference on Computer Graphics and Interactive Techniques, Addison-Wesley Reading, MA, 2000, pp. 417–424.

[5] A. Bertozzi, S. Esedoglu, and A. Gillette, *Inpainting of binary images using the Cahn–Hilliard equation*, IEEE Trans. Image Process., 16 (2007), pp. 285–291.

[6] A. Bertozzi, S. Esedoglu, and A. Gillette, *Analysis of a two-scale Cahn–Hilliard model for binary image inpainting*, Multiscale Model. Simul., 6 (2007), pp. 913–936.

[7] C. Braverman, *Photoshop Retouching Handbook*, IDG Books Worldwide, Foster City, CA, 1998.

[8] T.F. Chan, J. Shen, *Mathematical models for local non-texture inpaintings*. SIAM J. Appl. Math., 2002, 62, 1019–1043.

[9] T. F. Chan, S. H. Kang, and J. Shen, *Euler's elastica and curvature-based inpainting*, SIAM J. Appl. Math., 63 (2002), pp. 564–592.

[10] T.F. Chan, J. Shen, and S.H. Kang, *Non-texture inpainting by curvature-driven diffusions*, J. Visual Commun. Imag. Represenation 12 (2001), 436– 449.

[11] J.W. Cahn and J.E. *Hilliard, Free energy of a nonuniform system I. Interfacial free energy*, J. Chem. Phys. 28 (1958), 258–267.

[12] S. Esedoglu and R. March, *Segmentation with depth but without detecting junctions*, J. Math. Imag. Vision 18 (2003), 7–15.

[13] S. Esedoglu and J. Shen, *Digital inpainting based on the Mumford-Shah-Euler image model*, Eur. J. Appl. Math. 2000 (2000), 1–26.

[14] J. B. Greer and A. L. Bertozzi, *H1 solutions of a class of fourth order nonlinear equations for image processing*, Discrete Cont. Dyn. Systems 10 (2004), 349–366.

[15] J.B. Greer and A.L. Bertozzi, *Traveling wave solutions of fourth order PDE's for image processing*, SIAM J. Math. Anal. 36 (2004), 38–68.

[16] J. B. Greer, A. L. Bertozzi, and G. Sapiro, *Fourth order partial differential equations on general geometries*, J. Comput. Phys. 216 (2006), 216– 246.

[17] J. kim, C.O. Lee, *Three-Dimensional Volume Recon struction Using Two-Dimensional Parallel Slices*, SIAM J. IMAGING SCIENCES , 2019 Society for Industrial and Applied Mathematics Vol. 12, No. 1, pp. 1–27.

[18] D. King, *The Commissar Vanishes*, Henry Holt and Company, New York, 1997.

[19] S. Masnou and J. M. Morel, *Level lines based disocclution*, in Proceedings of the 5th IEEE International Conference on Image Processing, Vol. 3, 259–263, 1998.

[20] L. Rudin, S. Osher, and E. Fatemi, *Nonlinear total variation based noise removal algorithms*. Physica D, 60:259–268, 1992.

[21] L. Rudin and S.Osher, *Total variation based image restoration with free local constraints*. In International Conference on Image Processing, volume I, pages 31–35, November 1994.

[22] J. Shen, *Inpainting and the fundamental problem of image processing*, SIAM News 36, 1997.

[23] Tamizkar, M., Tavakkoli, A. and Matinfar, M., 2022. A new approach for image inpainting by modification on total variation model. *Journal of Interdisciplinary Mathematics*, *25*(6), pp.1665-1674.

[24] A. N. Tikhonovand V. Y. Arsenin. *Solutions of ill-posed problems*. Winston and Sons, Washington, D.C., 1977.

[25] S.Walden. *The Ravished Image*. St.Martin's Press, New York, 1985.